ARMY RESEARCH LABORATORY

Corrosion in Methylphosphonic Difluoride

Chester V. Zabielski and Milton Levy

ARL-TR-651

December 1994

The findings in this report are not to be construed as an official Department of the Army position unless so designated by other authorized documents.

Citation of manufacturer's or trade names does not constitute an official endorsement or approval of the use thereof.

Destroy this report when it is no longer needed. Do not return it to the originator.

REPORT DOCUMENTATION PAGE

Form Approved
OMB No. 0704-0188

1. AGENCY USE ONLY *(Leave blank)*	2. REPORT DATE	3. REPORT TYPE AND DATES COVERED
	December 1994	

4. TITLE AND SUBTITLE

Corrosion in Methylphosphonic Difluoride

5. FUNDING NUMBERS

6. AUTHOR(S)

Chester V. Zabielski* and Milton Levy*

7. PERFORMING ORGANIZATION NAME(S) AND ADDRESS(ES)

Army Research Laboratory
Watertown, MA 02172-0001
AMSRL-MA-CC

8. PERFORMING ORGANIZATION REPORT NUMBER

ARL-TR-651

9. SPONSORING/MONITORING AGENCY NAME(S) AND ADDRESS(ES)

10. SPONSORING/MONITORING AGENCY REPORT NUMBER

11. SUPPLEMENTARY NOTES

*Present affiliation - U.S. Army Research Laboratory, Watertown, MA 02172-0001

12a. DISTRIBUTION/AVAILABILITY STATEMENT

Approved for public release; distribution unlimited.

12b. DISTRIBUTION CODE

13. ABSTRACT *(Maximum 200 words)*

Electrochemical potentiodynamic polarization studies were conducted for a variety of ferrous and nonferrous metals in methylphosphonic difluoride. Studies were also made of the effects of organic inhibitors on the corrosion rates of 1020 steel (UNS G10200), type 316L (UNS S31603), and type 304 stainless steel (UNS S30400), and magnesium in methylphosphonic difluoride.

14. SUBJECT TERMS

Corrosion-resistant Alloys, Corrosion Inhibition, Methylphosphonic Difluoride, Electrochemical Tests

15. NUMBER OF PAGES

10

16. PRICE CODE

17. SECURITY CLASSIFICATION OF REPORT	18. SECURITY CLASSIFICATION OF THIS PAGE	19. SECURITY CLASSIFICATION OF ABSTRACT	20. LIMITATION OF ABSTRACT
Unclassified	Unclassified	Unclassified	UL

Corrosion in Methylphosphonic Difluoride

Chester V. Zabielski and Milton Levy
U.S. Army Research Laboratory, Watertown, MA 02172-0001

Electrochemical potentiodynamic polarization studies were conducted for a variety of ferrous and nonferrous metals in methylphosphonic difluoride. Studies were also made of the effects of organic inhibitors on the corrosion rates of 1020 steel (UNS G10200), type 316L (UNS S31603), and type 304 stainless steel (UNS S30400), and magnesium in methylphosphonic difluoride.

Chemical weapons in the United States include binary munitions in which two components are kept in separate compartments until activation. These munitions must be stockpiled for long periods of time (up to 30 years) and then must operate reliably when the need arises.

Very reliable storage containers are essential to the subsequent activation and availability of this weapon system. A storage container's failure is a hazard in itself because of the toxic constituents. The principal cause of failure will be corrosion of the storage container by the highly corrosive methylphosphonic difluoride (DF). This compound reacts with the alcohol in the weapon system and forms the active agent (GB). The hydroscopic DF interacts with water that may be present and forms hydrogen fluoride (HF). DF is not used in pure form but contains significant amounts of chlorides and cathodic impurities such as iron, copper, and nickel, which can increase corrosion rates of most metals and alloys. Although polymeric liners are used, they may slowly interact with the HF; therefore, the substrate metal/alloy must be able to withstand corrosion and pitting attack. Pitting attack could rapidly perforate the container. Vapor phase (thin electrolyte film) corrosion has been shown to be the primary failure mode in GB munitions and is prevalent in DF systems.

The objectives of this study were to:

- investigate the kinetics and mechanisms of corrosion of Al 6061-T6 (UNS A96061) and candidate metal alloys in DF,
- establish effective corrosion inhibitors, and
- ultimately incorporate or immobilize inhibitors into coatings that provide protection above the liquid line.

Experimental

Materials

The DF was used in two purities, 97.1 and 99.8%; the compositions are listed in Table 1. Organic inhibitors were added to DF to determine their effects on the corrosion processes and to protect the alloys against corrosion. A variety of metals and alloys were used.

Specimens and Procedures

The corrosion cell was a modified polarographic trielectrode cell constructed from polytetrafluoroethylene[1,2] The reference electrode in the DF solution was a silver wire in 0.1 M silver nitrate in acetonitrile. The working electrode was an alloy cylinder with a 1.2-cm^2 surface area. The counter electrode was a spiralled 40-gauge platinum wire. In order to describe the anodic and cathodic processes, anodic and cathodic polarization measurements were made utilizing the potential sweep method. The electrode potential was continuously changed at a constant rate of 5,000 mV/h, and current was simultaneously recorded. Corrosion rates in micrometers per year (μm/y) were generally determined by extrapolating the cathodic portion of the polarization curve to the corrosion potential; pitting scans were performed to elucidate the mechanisms of passivation or pitting. One-hour potential-time data were obtained for all alloys in all environments to determine the corrosion potentials. Modified polarization specimens of 1.2- to 4.5-cm^2 surface area were exposed for up to 180 days at room temperature to DF-22 vapor by positioning the specimen above the

TABLE 3

Potentiodynamic Corrosion Rates and Pitting Observations for Nonferrous Alloys in DF-2 (97.1%) and DF-22 (99.8%) at 25°C

Alloy	Corrosion Rate				Pitting in DF-22		
	DF-2		DF-22		Polarization		Exposure
	Cathodic (μm/y)	Anodic (μm/y)	Cathodic (μm/y)	Anodic (μm/y)	Scan	Visual	Vapor
Al 7075-T6	10.2	nd	1.5	1.7	N	N	nd
Al 5083	10.7	12.4	1.8	1.7	P	nd	PP
Al 2090	12.4	15	2.3	2.0	SP	SP	N
Al 2017	1.0	2	15.7	35.3	N	N	nd
Al 6061-T6	15	9.9	10	10	N	nd	PP
Al 4043	78.5	28	16.3	37.3	N	HP	N
Pure Cu	1,717	996	38.9	48.3	P	PP	nd
Cu (5% Zn)	nd	nd	50.8	71.6	P	nd	nd
Cu (30% Zn)	nd	nd	40.6	42.9	SP	SP	nd
Cu (30% Zn, 2% Pb)	600	1,159	7.1	77.7	P	PP	nd
Pure Mg	nd	nd	277.9	427.0	HP	P	HP
U (0.75% Ti) (warm worked)	nd	nd	129.5	136.1	SP	N	nd

Key for pitting data:
nd = no data PP = possible pitting P = pitting N = no pitting SP = slight pitting HP = heavy pitting

TABLE 4

Potentiodynamic Corrosion Rates and Pitting Observations for Ferrous and Nickel Alloys in DF-2 (97.1%) and DF-22 (99.8%) at 25°C

Alloy	Corrosion Rate				Pitting in DF-22		
	DF-2		DF-22		Polarization		Exposure
	Cathodic (μm/y)	Anodic (μm/y)	Cathodic (μm/y)	Anodic (μm/y)	Scan	Visual	Vapor
20 Cb3	nd	nd	7.6	5.6	N	N	nd
317L SS	nd	nd	30.5	29.8	N	N	nd
316L SS	938.3	1,956	6.9	8.4	N	PP	N
304 SS	1,104	1,122	4.1	6.1	SP	PP	HP
430 SS	nd	nd	18.5	23.1	PP	SP	nd
1020	2,506	3,452	444.5	528.1	N	nd	N
Hastelloy C	4.8	5.8	2.0	1.3	P	nd	PP
Hastelloy B	52.3	56.9	17.3	40.1	SP	nd	SP
Monel	380.2	933.9	46.0	62.2	PP	nd	nd
Ni 200	nd	nd	61.0	65.5	SP	PP	nd
Commercially pure Ni	nd	nd	35.1	22.4	P	PP	nd

Key for pitting data:
nd = no data PP = possible pitting P = pitting N = no pitting SP = slight pitting HP = heavy pitting

chloride ions at the anode and cation reduction of metallic impurities at the cathode. The 1020 steel had the highest corrosion rate in both solutions. Al 6061-T6, Hastelloy C, and Ta-10W had low corrosion rates of less than 25.4 μm/y in both solutions.

Polarization curves were obtained for several aluminum (Al) alloys in both DF solutions. These curves show that Al 7075-T6 (UNS A97075), Al 5083 (UNS A95083), Al 6061-T6, and Al 2090 (UNS A92090) develop passive regions in both solutions with current densities less than 20 μA/cm². Table 3 lists the corrosion rates determined from the extrapolation of the cathodic and anodic Tafel slopes to the corrosion potential. Al 7075-T6, Al 5083, Al 6061-T6, and Al 2090 have corrosion rates less than 25.4 μm/y in both DF-2 and DF-22 solutions. The remaining alloys, 4043 (UNS A94043) and 2017 (UNS A92017), exhibited slightly higher corrosion rates. Pitting scan data in Table 3 for the DF-22 solution indicated that Al 5083, which contains 4.5% magnesium, and Al 2090, which contains 2.4% lithium, experienced pitting.

Visual examination of the polarization specimens after the pitting scans showed evidence of pitting in Al 5083 and Al 4043. Table 3 also shows that Al 5083 and Al 6061-T6 pit when exposed to DF-22 vapor.

Examination of polarization curves for selected copper (Cu) alloys in DF-2 and DF-22 solutions showed that Cu alloys exhibited passive current densities (100 μA/cm²) in DF-22 but not in DF-2 solution. Adding zinc to Cu displaces the curves toward more negative potentials. The corrosion rates in DF-2 solution for Cu and the Cu alloy containing 38% zinc and 2% lead (UNS C36000) listed in Table 3 exceeded 600 μm/y, and are significantly higher than those for the Cu alloys in DF-22 solution. The corrosion rates in DF-22 solution were between 38.9 and 77.7 μm/y, except for Cu (38% zinc, 2% lead), which had a

TABLE 5
Potentiodynamic Corrosion Rates and Percent Inhibiting Efficiencies[A] of 1020 Steel in DF-2 (97.1%) with Organic Inhibitor Additions

Inhibitor Addition (0.025 M)	Cathodic		Anodic	
	(μm/y)	(I.E.%)[A]	(μm/y)	(I.E.%)[A]
DF-2	2,507	—	3,452	—
Sulfanilamide	645	74.3	546	84.2
Benzonitrile	856	65.8	1,085	68.6
Benzothiazole	913	63.6	1,275	63.1
Benzotriazole	1,105	56.0	1,603	53.6
NLS (Na salt)[B]	1,399	44.2	2,101	39.1
NLS (free acid)[B]	1,420	43.4	2,504	27.4
2-Benzothiazolethiol	1,478	41.0	2,705	21.6
Benzimidazole	—	—	2,995	13.2
1-Phenyl-2-Thiourea	1,824	27.2	3,454	0.0

[A]Inhibiting efficiencies = I.E.
[B]N-lauroyl sarcosine

TABLE 6
Potentiodynamic Corrosion Rates and Percent Inhibiting Efficiencies of 316L SS in DF-2 (97.1%) with Organic Inhibitor Additions

Inhibitor Addition (0.025 M)	Cathodic		Anodic	
	(μm/y)	(I.E.%)	(μm/y)	(I.E.%)
DF-2	1,105	—	1,123	—
Benzotriazole	27.4	97.5	16	98.6
NLS (free acid)[A]	653	40.8	295	73.8
NLS (Na salt)[A]	770	30.4	353	68.6
Benzothiazole	787	28.6	523	63.6

[A] N-lauroyl sarcosine

rate of 7.1 μm/y. Pitting scan data in Table 3 for the DF-22 solution disclosed that pitting occurred. Visual examination of the polarization specimens after the completion of the pitting scans confirmed that pitting did indeed occur.

Compared to Al 6061-T6 and Al 2017 analysis of the polarization curves for commercially pure magnesium (Mg), U-0.75% Ti (warm worked), which was solution treated in vacuum at 850°C, vertically water quenched, and warm rod rolled 33.4% at 250°C, showed that Mg and U-0.75% Ti exhibited in DF-22 solution more active corrosion potentials and higher current densities, but passive current densities did not exceed 100 μA/cm. Passive current densities for the Al alloys were between 5 and 10 μA/cm^2. The corrosion rates in DF-22 solution of commercially pure Mg and U-0.75% Ti significantly exceeded the rates for Al 6061-T6 and Al 2017, but were lower than those for 1020 steel (Tables 3 and 4). Pitting scan data for commercially pure magnesium in DF-22 solution indicated severe pitting occurred; slight pitting occurred on warm worked U-0.75% Ti. Visual examination of the polarization specimens after completion of the pitting scans confirmed the occurrence of pitting in commercially pure Mg. DF-22 (99.8%) vapor exposure data also showed severe pitting of Mg.

Polarization curves for stainless steel (SS) and other ferrous alloys in DF-22 (99.8%) solution showed that the higher chromium and nickel content of SS displaced the 1020 steel curve toward more noble potentials and lower current densities. The corrosion rates for types 304 SS (UNS S30400) and 316L SS (UNS S31603) in DF-2 solution markedly exceeded those in DF-22 solution but were lower than the corrosion rates for 1020 steel. Pitting scan data in Table 4 indicates that slight pitting occurred on types 304 SS and 430 SS (UNS 43000) in the DF-22 solution. Visual examination of polarization specimens after completion of pitting scans disclosed slight pitting for types 430 SS, 304 SS, and 316L SS. The DF-22 vapor exposure data in Table 4 indicates severe pitting of 304 SS, but no pitting of 316L SS.

Comparing polarization curves for nickel (Ni) alloys in DF-22 solution with pure Ni, it appears that adding chromium and molybdenum to Ni displaced the curves for Hastelloy B and Hastelloy C toward more noble potentials and lower current densities. The addition of Cu to pure Ni shifts the curve for Monel toward more negative or active potentials. Corrosion rates in DF-22 solution, in order of increasing rates, were Hastelloy C (2.0 μm/y), Hastelloy B (17.3 μm/y), commercially pure Ni (35.1 μm/y), Monel (46 μm/y), and Ni 200 (61 μm/y). Corrosion rates in DF-2 solution were somewhat higher than in DF-22 for Hastelloy C (4.8 μm/y) and Hastelloy B (52.3 μm/y), and markedly higher for Monel (380.2 μm/y). Pitting scan data in Table 4 indicates that Hastelloy C, Hastelloy B, Ni 200, Monel, and commercially pure Ni undergo pitting in the DF-22 solution. The visual examination of polarization specimens after completion of the pitting scans revealed pitting of Ni 200 and commercially pure Ni. DF-22 vapor exposure data in Table 4 indicates pitting of Hastelloy B and Hastelloy C.

Inhibitor Studies

Table 5 lists the percent cathodic and anodic inhibition efficiencies of several organic compounds in reducing the corrosion rate of mild steel in DF-2 solutions. The inhibition is based on corrosion rates determined from cathodic and anodic Tafel slope extrapolations which do not account for pitting. Sulfanilimide was found to have the highest cathodic and anodic inhibiting efficiencies of 74.3 and 84.2%, respectively. Benzonitrile, benzothiazole, and benzotriazole additions provided cathodic and anodic inhibiting efficiencies greater than 50%. Sulfanilimide, benzonitrile, and

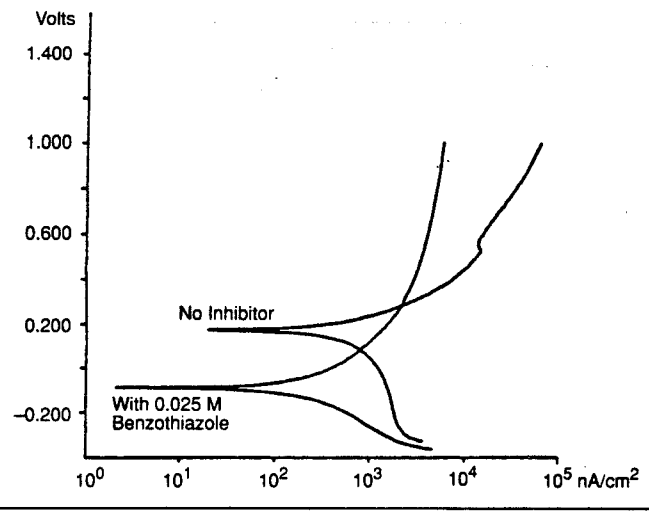

FIGURE 2
Effect of 0.025 M benzothiazole on potentiodynamic polarization curves for 304 SS in DF-22 (99.8%) at 25°C. Scan rate: 1.388 mV/s.

benzotriazole are nitrogen (N)-containing additives, while benzothiazole is a sulfur (S)-containing additive. These species may chemically absorb on the surface to inhibit corrosion by acidic fluorides (hydrogen fluoride) and acidic chlorides (hydrochloric acid). The remaining organic inhibitor additions of NLS (Na salt), NLS (free acid), benzimidazole (N-containing additives), and 2-benzothiazole-ethiol and 1-phenyl-2-thiourea (S-containing additives) had cathodic and anodic inhibiting efficiencies lower than 50%.

Table 6 contains similar data for type 316L SS. Benzotriazole had the highest cathodic and anodic inhibiting efficiencies of 97.5 and 98.6%, respectively, but pitting scan data and visual examination showed that pitting occurred. Since comparable polarization data and visual examination of 316L SS exposed to DF-2 solution without an inhibitor showed no evidence of pitting, it is clear that benzotriazole will induce pitting of 316L SS despite the excellent inhibition displayed. NLS (free acid) gave the next highest cathodic and anodic inhibiting efficiencies of 40.8 and 73.8%, respectively.

Figure 2 compares anodic polarization curves for type 304 SS in DF-22 with and without a 0.025 M benzothiazole addition. The inhibitor addition shifted the curve toward more negative potentials and lower current densities, and reduced the passive current density from 80 to 8 $\mu A/cm^2$. Table 7 compares the efficacy of the four inhibitors for 304 SS in DF-22. Benzotriazole had the highest cathodic inhibiting efficiency of 76.4%, followed by benzothiazole and sulfanilimide (greater than 50%) and the Na-salt of n-lauroyl sarcosine

TABLE 7
Potentiodynamic Corrosion Rates and Percent Inhibiting Efficiencies of 304 SS in DF-22 with Organic Inhibitors Added

	Inhibitor Efficiency				Pitting Observations			
	Anodic		Cathodic		Polarization		Exposure	
Inhibitor	(μm/y)	(I.E.%)	(μm/y)	(I.E.%)	Scan	Visual	Liquid	Vapor
No inhibitor, 0.025 M	8.36	—	6.86	—	SP	PP	HP	HP
Benzotriazole, 0.025 M	2.46	70.5	1.63	76.4	N	N	nd	nd
Benzothazole, 0.025 M	2.44	70.8	2.11	69.6	N	N	N	N
Sulfanilamide, 0.025 M	4.17	50.2	3.30	52.0	N	N	nd	nd
N-lauroyl sarcosine (Na salt)	4.70	43.8	4.14	39.9	N	N	nd	nd

Key for pitting data:
nd = no data PP = possible pitting P = pitting N = no pitting SP = slight pitting HP = heavy pitting

TABLE 8
Potentiodynamic Corrosion Rates and Percent Inhibiting Efficiencies of Commercially Pure Mg in DF-22 with Organic Inhibitors Added

	Inhibitor Efficiency				Pitting Observations		
	Cathodic		Anodic		Polarization		Exposure
Inhibitor	(μm/y)	(I.E.%)	(μm/y)	(I.E.%)	Scan	Visual	Vapor
No inhibitor, 0.025 M	277.9	—	427	—	P	HP	HP
Benzothiazole, 0.025 M	34.8	87.5	—	nf	N	SP	P
Benzotriazole, 0.025 M	78.2	71.7	96	77.5	N	SP	nd

Key for pitting data:
nd = no data nf = not found P = pitting N = no pitting SP = slight pitting HP = heavy pitting

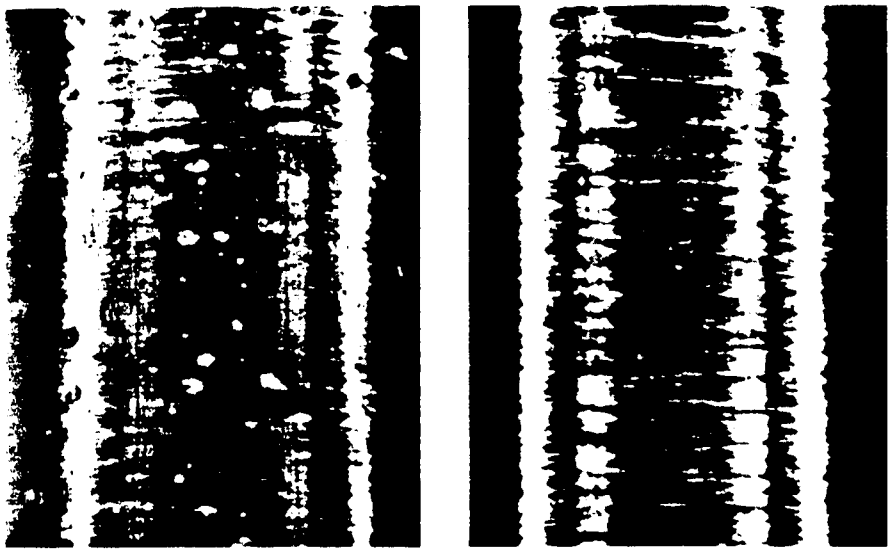

(a) (b)

FIGURE 3

Elimination of pitting of type 304 SS exposed to DF-22 vapor for 30 days by addition of 0.025 M benzothiazole. Original magnification 32x; reduced. (a) type 304 SS in DF-22 vapor. (b) type 304 SS in DF-22 vapor with 0.025 M benzothiazole.

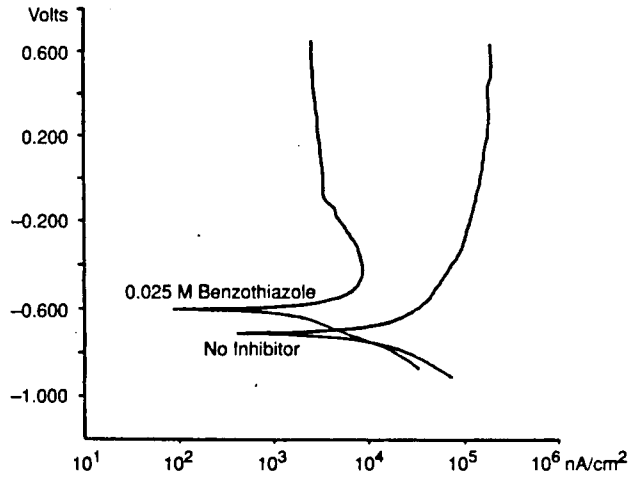

FIGURE 4

Effect of organic inhibitors on potentiodynamic polarization behavior of commercially pure Mg in DF-22 (99.8%) at 25°C. Scan rate: 1.388 mV/s.

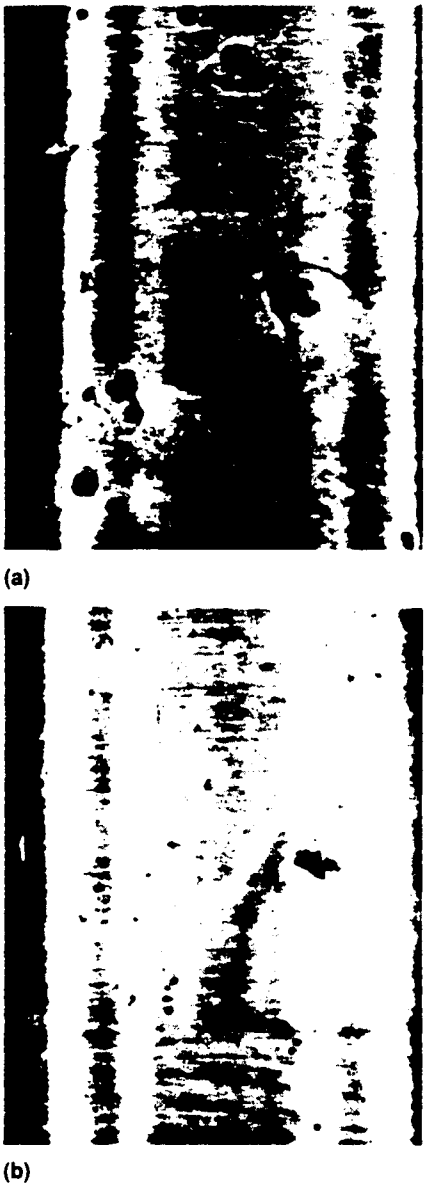

(a) (b)

FIGURE 5

Reduction of pitting of commercially pure Mg exposed to DF-22 vapor for 15 days by addition of 0.025 M benzothiazole. Original magnification 32x; reduced. (a) Commercially pure Mg in DF-22 vapor. (b) Commercially pure Mg in DF-22 vapor with 0.025 M benzothiazole.

(below 50%). Pitting scan data (Table 7) show that all the inhibitor additions eliminated pitting. Visual examination of the polarization specimens confirmed the elimination of pitting by the four inhibitors. Figure 3 shows that 304 SS specimens exposed to the vapor above the DF-22 (99.8%) solution with 0.025 M benzothiazole were free of pitting.

Figure 4 compares anodic polarization curves for commercially pure Mg in DF-22 (99.8%) with and without 0.025 M benzothiazole. The addition of the inhibitor shifted the curve toward more noble potentials, showed an active-passive transition, and reduced the critical current density for passivity from 100 to 10 μA/cm². Table 8 shows that benzothiazole had a higher cathodic inhibiting efficiency (87.5%) than benzotriazole (71.5%). The pitting scan data (Table 8) show that both inhibitors eliminated pitting. Visual examination of the polarization specimens after pitting scans, however, revealed that slight pitting was evident. Figure 5 shows that commercially pure Mg specimens exposed to the vapor above the DF-22 (99.8%) solution with 0.025 M benzothiazole had a very large reduction in the extent and size of pitting.

Conclusions

The corrosion rates of the metals/alloys in 97.1% DF were significantly higher than in 99.8% DF. The

impurities in the 97.1% solution probably contributed to the increase in the corrosion rate. The 1020 steel had the highest corrosion rate in both solutions. Hastelloy C, Ta-10W, Al 6061T6, Al 5083, Al 2090, and Al 7075-T6 had corrosion rates of less than 25.4 μm/y in both solutions.

The corrosion potentials of the metals/alloys were generally more active in the higher purity solution, except for Hastelloy B, Hastelloy C, types 304 SS and 316L SS, Al 2090, Al 2017, and Cu (38% zinc, 2% lead).

Pitting tendency, as determined from potentiodynamic pitting scans, disclosed that pitting did not occur for any metal/alloy in the 97.1% solution, but that pitting did occur in the higher purity 99.8% solution for most alloys.

The best inhibitor for specific alloys in DF is as follows: Sulfanilimide for 1020 steel and benzotriazole for 316L SS in 97.1% DF; benzotriazole for 304 SS and benzothiazole for magnesium in 99.8% DF.

Potentiodynamic pitting scans for type 304 SS in 99.8% DF solution with 0.025 M additions of benzotriazole, benzothiazole, sulfanilimide, or N-lauroyl sarcosine (Na salt), and for Mg with benzothiazole or benzotriazole additions showed that these inhibitors reduced or eliminated pitting. An addition of 0.025 M benzothiazole to the liquid phase greatly reduced the extent of pitting of type 304 SS and Mg specimens after long-term exposure to vapor above 99.8% DF.

References

1. P.A. Tarantino, M.M. Decker, "Use of Electrochemical Techniques to Study the Corrosion of Selected Alloys by DF," U.S. Army Chemical Research, Development, and Engineering Center, CRDC T 84032, July 1984.
2. C.V. Zabielski, M. Levy, Corrosion on Metals/Alloys in Methylphosphonic Difluoride. Extended Abstracts of the Electrochemical Society, vol. 347, 1986, p. 86.

More information is available in paper no. 544, presented at CORROSION/94 in Baltimore, Maryland.

DISTRIBUTION LIST

No. of Copies	To
1	Office of the Under Secretary of Defense for Research and Engineering, The Pentagon, Washington, DC 20301
	Director, U.S. Army Research Laboratory, 2800 Powder Mill Road, Adelphi, MD 20783-1197
1	ATTN: AMSRL-OP-SD-TP, Technical Publishing Branch
1	AMSRL-OP-SD-TA, Records Management
1	AMSRL-OP-SD-TL, Technical Library
	Commander, Defense Technical Information Center, Cameron Station, Building 5, 5010 Duke Street, Alexandria, VA 23304-6145
2	ATTN: DTIC-FDAC
1	MIA/CINDAS, Purdue University, 2595 Yeager Road, West Lafayette, IN 47905
	Commander, Army Research Office, P.O. Box 12211, Research Triangle Park, NC 27709-2211
1	ATTN: Information Processing Office
	Commander, U.S. Army Materiel Command, 5001 Eisenhower Avenue, Alexandria, VA 22333
1	ATTN: AMCSCI
	Commander, U.S. Army Materiel Systems Analysis Activity, Aberdeen Proving Ground, MD 21005
1	ATTN: AMXSY-MP, H. Cohen
	Commander, U.S. Army Missile Command, Redstone Arsenal, AL 35809
1	ATTN: AMSMI-RD-CS-R/Doc
	Commander, U.S. Army Armament, Munitions and Chemical Command, Dover, NJ 07801
1	ATTN: Technical Library
	Commander, U.S. Army Natick Research, Development and Engineering Center Natick, MA 01760-5010
1	ATTN: SATNC-MI, Technical Library
	Commander, U.S. Army Satellite Communications Agency, Fort Monmouth, NJ 07703
1	ATTN: Technical Document Center
	Commander, U.S. Army Tank-Automotive Command, Warren, MI 48397-5000
1	ATTN: AMSTA-ZSK
1	AMSTA-TSL, Technical Library
	President, Airborne, Electronics and Special Warfare Board, Fort Bragg, NC 28307
1	ATTN: Library
	Director, U.S. Army Research Laboratory, Weapons Technology, Aberdeen Proving Ground, MD 21005-5066
1	ATTN: AMSRL-WT
2	Technical Library

No. of Copies	To
	Commander, Dugway Proving Ground, UT 84022
1	ATTN: Technical Library, Technical Information Division
	Commander, U.S. Army Research Laboratory, 2800 Powder Mill Road, Adelphi, MD 20783
1	ATTN: AMSRL-SS
	Director, Benet Weapons Laboratory, LCWSL, USA AMCCOM, Watervliet, NY 12189
1	ATTN: AMSMC-LCB-TL
1	AMSMC-LCB-R
1	AMSMC-LCB-RM
1	AMSMC-LCB-RP
	Commander, U.S. Army Foreign Science and Technology Center, 220 7th Street, N.E., Charlottesville, VA 22901-5396
3	ATTN: AIFRTC, Applied Technologies Branch, Gerald Schlesinger
	Commander, U.S. Army Aeromedical Research Unit, P.O. Box 577, Fort Rucker, AL 36360
1	ATTN: Technical Library
	U.S. Army Aviation Training Library, Fort Rucker, AL 36360
1	ATTN: Building 5906-5907
	Commander, U.S. Army Agency for Aviation Safety, Fort Rucker, AL 3636
1	ATTN: Technical Library
	Commander, Clarke Engineer School Library, 3202 Nebraska Ave., N., Fort Leonard Wood, MO 65473-5000
1	ATTN: Library
	Commander, U.S. Army Engineer Waterways Experiment Station, P.O. Box 631, Vicksburg, MS 39180
1	ATTN: Research Center Library
	Commandant, U.S. Army Quartermaster School, Fort Lee, VA 23801
1	ATTN: Quartermaster School Library
	Naval Research Laboratory, Washington, DC 20375
1	ATTN: Code 6384
	Chief of Naval Research, Arlington, VA 22217
1	ATTN: Code 471
	Commander, U.S. Air Force Wright Research and Development Center, Wright-Patterson Air Force Base, OH 45433-6523
1	ATTN: WRDC/MLLP, M. Forney, Jr.
1	WRDC/MLBC, Mr. Stanley Schulman
	U.S. Department of Commerce, National Institute of Standards and Technology, Gaithersburg, MD 20899
1	ATTN: Stephen M Hsu, Chief, Ceramics Division, Institute for Materials Science and Engineering

No. of Copies	To
1	Committee on Marine Structures, Marine Board, National Research Council, 2101 Constitution Avenue, N.W., Washington, DC 20418
1	Materials Sciences Corporation, Suite 250, 500 Office Center Drive, Fort Washington, PA 19034
1	Charles Stark Draper Laboratory, 555 Technology Square, Cambridge, MA 02139
1	General Dynamics, Convair Aerospace Division, P.O. Box 748, Fort Worth, TX 76101 ATTN: Mfg. Engineering Technical Library
1	Plastics Technical Evaluation Center, PLASTEC, ARDEC, Bldg. 355N, Picatinny Arsenal, NJ 07806-5000 ATTN: Harry Pebly
1	Department of the Army, Aerostructures Directorate, MS-266, U.S. Army Aviation R&T Activity - AVSCOM, Langley Research Center, Hampton, VA 23665-5225
1	NASA - Langley Research Center, Hampton, VA 23665-5255
1	U.S. Army Vehicle Propulsion Directorate, NASA Lewis Research Center, 2100 Brookpark Road, Cleveland, OH 44135-3191 ATTN: AMSRL-VP
1	Director, Defense Intelligence Agency, Washington, DC 20340-6053 ATTN: ODT-5A, Mr. Frank Jaeger
1	U.S. Army Communications and Electronics Command, Fort Monmouth, NJ 07703 ATTN: Technical Library
1	U.S. Army Research Laboratory, Electronic Power Sources Directorate, Fort Monmouth, NJ 07703 ATTN: Technical Library
2 5	Director, U.S. Army Research Laboratory, Watertown, MA 02172-0001 ATTN: AMSRL-OP-WT-IS, Technical Library Author